



# Kashf Journal of Multidisciplinary Research

Vol: 02 - Issue 06 (2025)

P-ISSN: 3007-1992 E-ISSN: 3007-200X

https://kjmr.com.pk

# APPLICATION OF A HYBRID B-SPLINE METHOD FOR THE NUMERICAL ANALYSIS OF TIME-FRACTIONAL DIFFUSION WAVE EQUATION

\*Sagar Hassan<sup>1</sup>, Muhammad Amin<sup>2</sup>, Saima Mushtaq<sup>3</sup>

\*1,2,3 Faculty of Sciences, The Superior University, Lahore, Pakistan

\*Corresponding author: (Sagarhassan70@gmail.com)

# **Article Info**



# **Abstract**

In this article, approximate solutions of Time-Fractional Diffusion Wave Equation has been investigated using a hybrid cubic B-spline technique with finite difference scheme. For the discretization of time fractional derivative Caputo-Fabrizo formula is employed. To get the numerical out comes the Caputo-Fabrizo fractional derivative and a hybrid cubic B-spline strategy is delved. The presented method is proved to be unconditionally stable with a second order convergence. The proposed scheme is validated using some test problems, demonstrating its feasibility and reasonable accuracy. Numerical results show that the applied method is efficient and computationally economic in solving the time-fractional Diffusion Wave Equation.



This article is an open access article distributed under the terms and conditions of the Creative Commons Attribution (CC BY) license

https://creativecommons.org/licenses/by/4.0

# **Keywords:**

Stability, Convergence, Diffusion Wave Equation, Caputo Fabrizio fractional operator, Hybrid Cubic B-Spline (HCBS).

### 1. Introduction

Fractional calculus (FC) studies differentiation and integration of fractional orders. This field has gained popularity in recent decades. A brief discussion on this topic is presented in [1,2]. FC is respected for its many scientific and engineering uses. FC is used in control theory [3], viscoelastic flow [4], continuum mechanics [5], tumor growth modeling [6], transport phenomena [7], random walk analysis [8], turbulence studies [9,10], coronavirus research [11,12] and the analysis of dynamical systems [13,14]. Fractional integrals and derivatives can express the memory and genetic properties of many materials and processes, especially those affected by irregular diffusion, according to several academics [15,16]. Fractional partial differential equations (FPDEs) sometimes indicate fractional problems more precisely than integer-order approximations. However, most FPDEs cannot be solved accurately. Thus, a lot of research article has focused on numerical solutions to these difficulties. This study will explore (TFDWE) with damping and reactivity variables to find numerical solutions for various circumstances.

$$\frac{\partial^{\alpha} y(v,t)}{\partial t^{\alpha}} + \phi \frac{\partial y(v,t)}{\partial t} + \psi y(v,t) - \frac{\partial^{2} y(v,t)}{\partial v^{2}} = q(v,t), \alpha \in (1,2], v \in [a,b], t \in [t_{0},T], \quad (1)$$

With initial conditions (ICS):

$$y(v,t_0) = \omega_1(v), \qquad y_t(v,t_0) = \omega_2(v), \tag{2}$$

$$y(a,t) = \psi_1(t), \qquad y(b,t) = \psi_2(t),$$
 (3)

where  $\phi$  and  $\psi$  are coefficients of the damping and reaction terms, respectively. q(v,t) is the source term and  $y_t(v,t_0)$  is a differentiable function of y(v,t) for time t at  $t=t_0$ . The fractional

derivative is in the form of Caputo-Fabrizio  $\frac{\partial^{\alpha}}{\partial t^{\alpha}}y(v,t)$  is described

$$\frac{\partial^{\alpha}}{\partial t^{\alpha}}y(v,t) = \frac{R(\alpha)}{2-\alpha} \int_{0}^{t} \frac{\partial^{2}}{\partial z^{2}} y(v,z) \exp\left[-\frac{\alpha}{2-\alpha}(t-z)\right] dz \tag{4}$$

In the Equation (4) R()  $\alpha$  refers to the normalization operator and satisfies that R R (0) (1) 1 = = . Where  $\alpha$  is the fractional derivative and shows the behavior of the equation, it means when  $\alpha$  = 1 Equation (1) becomes the diffusion equation,  $0 < \alpha \le 1$  Eq turns to the fractional diffusion equation or sub-diffusion equation. When  $\alpha$  = 2 it becomes a wave equation and  $1 < \alpha \le 2$  then the equation becomes a fractional wave equation.

# 1.1 Literature Review

The idea of fractional calculus emerged when differentiation and integration were applied to groups that were not integers. Fractional derivatives explain memory, engineering and physical system inheritance better than integer-order differentiation. Du et al [17] investigated fractional differentiation in response to L'Hôpital's issue. However, Kilbas et al [18] developed a strong mathematical framework for it, which advanced the area. The use of Caputo-Fabrizio fractional derivative has been studied in several articles. An analytical formula for the Gaussian-based CFFD, which focuses on the application in signal processing, has been developed by [19].

When dealing with nonlinear and nonhomogeneous cases, it is important to observe that FDWE does not have closed-form solution. Popular methods like Laplace transform, Green's function, Fourier order, eigenfunction expansion and separation of variables cannot correctly solve many fractional partial differential equations in many physical phenomenon. As a result, approximate numerical techniques are necessary to address such issues.

Numerous research articles have explored various numerical techniques for solving TFDWE. In recent years, researchers have developed many numerical methods to solve (TFDWE). Ding & Li

[20] proposed two computational methods for addressing TFDWEs with reaction terms. Avazzadeh et al [21] solved TFDWE using radial basis functions. Khader & Adel [22] introduced an algorithm based on Hermite formulas for fractional wave equations (FWEs). Chatterjee et al

[23] developed a method using Bernstein polynomials to solve nonlinear TFDWEs. Hooshmandasl et al [24] applied Legendre wavelets to address slow diffusion in fractional order and fractional diffusion wave equation in temporal direction. Ali et al [25] used an implicit difference technique to compute solutions for TFDWEs. F. Zhou & Xu [26] applied Chebyshev wavelets collocation technique to explore TFDWE.

For the time fractional diffusion-wave model, one conditionally stable finite difference scheme and two second-order stable schemes are suggested by Zeng [27]. Fundamental solutions to the fractional-order diffusion-wave problem have been found by Pskhu [28]. TFDWE under Neumann boundary-value constraints in a half-plane have been studied by Povstenko [29].

Ren and Sun [30] solved the multi-term time fractional diffusion-wave issue numerically efficiently using a compact finite difference technique with fourth-order accuracy. Sweilam et al [31] used the Crank-Nicolson finite difference approach to tackle the diffusion problem in time fractional order. Fractional diffusion-wave equations were solved using a unique iterative method by Daftardar-Gejji and Bhalekar [32]. Garg and Manohar [33] have used the matrix approach to produce a numerical solution of the fractional diffusion-wave equation with two spatial variables, while Khader [34] has written an article on the numerical solution for the fractional diffusion equation. The wavelets technique for the TFDWE was suggested by Heydari et al [35].

A TFDWE with reaction effect and estimated results are found in this study using an effective numerical scheme based on (HCBS) functions. The Caputo derivative in time fractional order is first discretized using the standard finite difference formula and then spatial derivatives are approximated using the θ-weighted scheme and (HCBS). Because of their minimal support and *C*2 continuity, (HCBS) functions offer more accuracy than standard finite difference techniques. The results obtained from numerical experiments are compared with those of [22] and [36]. The technique discussed in [22] has accuracy of 10<sup>-5</sup>, while the given scheme has an accuracy up to 10<sup>-9</sup> and 10<sup>-10</sup>, according to the comparison. It is demonstrated that the proposed technique is stable unconditionally. The presented scheme's convergence analysis is also covered. The algorithm's effectiveness and accuracy are validated by numerical experiments.

This paper's outline is as follows. In Section 2, Preliminaries and HCBS function is presented. The numerical scheme of TFDWE using Hybrid Cubic B-spline is described in section 3 and in section 4 and 5 stability and convergence is stated respectively. In section 6, the efficiency and stability of the scheme and results are discussed. Concluding remarks are discussed in the last section.

# 2. Preliminaries

**Definition 1. If**  $h \in L^2[a,b]$ , then PI is defined as [37]:

$$\sum_{m=-\infty}^{\infty} \left| \hat{h}(m) \right|^2 = \int_a^b \left| \tilde{h}(v) \right|^2 dv \tag{5}$$

The Fourier transform for all numbers m is shown by  $\hat{h}(m) = \int_{0}^{b} h(v) e^{2\pi i m v} dv$ 

# 2.1 Hybrid Cubic B-spline function

Consider  $a = v_0 < v_1 < \dots < v_N = b$  comprise the division of [a, b] corresponding with it at the nodes  $v_r = v_0 + rh$ ,  $r = 0,1,2,3 \dots N$ , where  $h = \frac{b-a}{N}$ . The definition of a Hybrid Cubic B-spline function is as

$$u(v_r) = \sin\left(\frac{v - v_r}{2}\right), \ q(v_r) = \sin\left(\frac{v_r - v}{2}\right), \ \varpi = \sin\left(\frac{h}{2}\right)\sin(h)\sin\left(\frac{3h}{2}\right)$$
 and  $b \in R$ . Where  $b$  is a free

parameter which controls the nature of Eq. (6). HCBS reduces to Cubic Trigonometric B-Spline (CTBS) when b = 0 and if b = 1 then it reduces to Cubic B-Spline (CBS). The CBS is geometrically invariant, convex, symmetric, dividing unity, and non-negative [38]. Furthermore,  $S_{-1}, S_{0,.....}S_{N+1}$  have also been formulated. For y(v,t), Regarding HCBS, the approximation Y(v,t) can be thought of as [39].

$$S_{r}^{4}(v) = \frac{b}{6h^{3}} \left\{ (v - v_{r})^{3} + \frac{1 - b}{\varpi} u^{3}(v_{r}) & v \in [v_{r}, v_{r+1}] \right\}$$

$$\begin{cases} \frac{b}{6h^{3}} \left\{ h^{3} + 3h^{2}(v - v_{r+1}) + 3h(v - v_{r+1})^{2} - 3(v - v_{r+1})^{3} \right\} & v \in [v_{r+1}, v_{r+2}] \right\}$$

$$\left\{ \frac{1 - b}{\varpi} \left\{ u(v_{r}) \left( u(v_{r})q(v_{r+2}) + q(v_{r+3})u(v_{r+1}) \right) + q(v_{r+4})u^{2}(v_{r+1}) \right\} \right\}$$

$$\begin{cases} \frac{b}{6h^{3}} \left\{ h^{3} + 3h^{2}(v_{r+3} - v) + 3h(v_{r+3} - v)^{2} - 3(v_{r+3} - v)^{3} \right\} & v \in [v_{r+2}, v_{r+3}] \right\} \\ + \frac{1 - b}{\varpi} \left\{ q(v_{r+4}) \left( u(v_{r+1})q(v_{r+3}) + q(v_{r+4})u(v_{r+2}) \right) + u(v_{r})q^{2}(v_{r+3}) \right\} \\ \frac{b}{6h^{3}} \left( v - v_{r} \right)^{3} + \frac{1 - b}{\varpi} u^{3}(v_{r}) & v \in [v_{r+3}, v_{r+4}] \\ 0 & otherwise \end{cases}$$

$$(6)$$

The approximate solution is

$$Y(v,t) = \sum_{r=-1}^{N+1} \mathcal{G}_r(t) S_r^4(v), \tag{7}$$

At each stage of time, control points  $\mathcal{G}_r(t)$  need to be found. At the nodal points, equations (6) and (7) give us the following close approximations:

$$\begin{cases} Y(v,t) = (Y)_r = \lambda_1 \mathcal{G}_{r-1} + \lambda_2 \mathcal{G}_r + \lambda_1 \mathcal{G}_{r+1} \\ Y_v(v,t) = (Y_v)_r = \lambda_3 \mathcal{G}_{r-1} + 0 \mathcal{G}_r + \lambda_4 \mathcal{G}_{r+1} \\ Y_{vv}(v,t) = (Y_{vv})_r = \lambda_5 \mathcal{G}_{r-1} + \lambda_6 \mathcal{G}_r + \lambda_5 \mathcal{G}_{r+1} \end{cases}$$
(8)

The values of  $S_r^4(v)$  and its derivatives at  $v = v_r$  are given by

$$S_r^4(v) = \begin{cases} \lambda_1 = \frac{b}{6} + (1-b)\sin^2\left(\frac{h}{2}\right)\cos ec(h)\cos ec\left(\frac{3h}{2}\right) \\ \lambda_2 = \frac{2b}{3} + (1-b)\frac{2}{1+2\cos(h)} \end{cases}$$

$$\frac{d}{dv}S_r^4(v) = \begin{cases} \lambda_3 = -\left(\frac{b}{2h} + (1-b)\frac{3}{4}\cos ec(\frac{3h}{2})\right) \\ \lambda_4 = \left(\frac{b}{2h} + (1-b)\frac{3}{4}\cos ec(\frac{3h}{2})\right) \end{cases}$$

$$\frac{d^{2}}{dv^{2}}S_{r}^{4}(v) = \begin{cases}
\lambda_{5} = \frac{b}{h^{2}} + (1-b)\frac{3(1+3\cos(h)\cos ec^{2}(h/2))}{16(2\cos(h/2) + \cos(3h/2))} \\
\lambda_{6} = -\left(\frac{2b}{h^{2}} + (1-b)\frac{3\cos^{2}(h/2)\cos ec^{2}(h/2)}{(2+4\cos(h))}\right)
\end{cases} \tag{9}$$

# 3. Description of numerical scheme

Take the range [0, T] and divide it into M equal parts of size  $\Delta t = \frac{1}{M}$  using the grid points  $0 = t_0 < t_1 < \dots < t_M = T$ , where  $t_n = n\Delta t$ ,  $n = 0,1,2\dots,M$ . Here's how to describe the CFFD of TFDWE at  $t = t_{n+1}$  as

$$\frac{\partial^{\alpha}}{\partial t^{\alpha}} y(v, t_{n+1}) = \frac{R(\alpha)}{2 - \alpha} \int_{0}^{t_{n+1}} \frac{\partial^{2}}{\partial z^{2}} y(v, z) \exp\left[-\frac{\alpha}{2 - \alpha} (t_{n+1} - z)\right] dz$$

$$= \frac{R(\alpha)}{2 - \alpha} \sum_{s=0}^{n} \int_{0}^{t_{n+1}} \frac{\partial^{2}}{\partial z^{2}} y(v, z) \exp\left[-\frac{\alpha}{2 - \alpha} (t_{n+1} - z)\right] dz$$
(10)

Using forward difference approach, Eq (10) becomes

$$= \frac{R(\alpha)}{2 - \alpha} \sum_{s=0}^{n} \frac{y(v, t_{s+1}) - 2y(v, t_{s}) + y(v, t_{s-1})}{(\Delta t)^{2}} \times \int_{0}^{t_{s+1}} \exp\left[-\frac{\alpha}{2 - \alpha}(t_{n+1} - z)\right] dz + \Phi_{\Delta t}^{n+1}$$

$$= \frac{R(\alpha)}{\alpha (\Delta t)^{2}} \left[1 - \exp(-\frac{\alpha}{2 - \alpha} \Delta t)\right] \sum_{s=0}^{n} [y(v, t_{n-s+1}) - 2y(v, t_{n-s}) + y(v, t_{n-s-1}) \exp(-\frac{\alpha}{2 - \alpha} s \Delta t) + \Phi_{\Delta t}^{n+1}$$

Hence

$$\frac{\partial^{\alpha}}{\partial t^{\alpha}}y(v,t_{n+1}) = \frac{\eta R(\alpha)}{\alpha(\Delta t)^{2}} \sum_{s=0}^{n} k_{s} [y(v,t_{n-s+1}) - 2y(v,t_{n-s}) + w(v,t_{n-s-1})] + \Phi_{\Delta t}^{n+1}$$
(11)

Where  $\eta = 1 - \exp(-\frac{\alpha}{2 - \alpha} \Delta t)$  and  $k_s = \exp(-\frac{\alpha}{2 - \alpha} s \Delta t)$ . Moreover the truncation error  $\Phi_{\Delta t}^{n+1}$  is given as

$$\left|\Phi_{\Delta t}^{n+1}\right| \le F(\Delta t)^2 \tag{12}$$

Where F is a constant. It can be checked that

- $k_s > 0$  and  $k_0 = 1, s = 0,1,2,3 ...., n$ ,
- $k_0 > k_1 > k_2 > \dots > k_s, k_s \to 0 \text{ as } s \to \infty$

$$\sum_{s=0}^{n} (k_s - k_{s+1}) = (1 - k_1) + \sum_{s=1}^{n} (k_s - k_{s+1}) + k_n = 1.$$

Using (11) and  $\theta$ -weighted scheme, Eq (1) becomes

$$\frac{\eta R(\alpha)}{\alpha (\Delta t)^{2}} \sum_{s=0}^{n} \left[ k_{s} \left[ y(v, t_{n-s+1}) - 2y(v, t_{n-s}) + y(v, t_{n-s-1}) \right] + \frac{\phi}{\Delta t} \left[ y(v, t_{n+1}) - y(v, t_{n}) \right] + \theta \left[ \psi y(v, t_{n+1}) - y_{vv}(v, t_{n+1}) \right] + (1 - \theta) \left[ \psi y(v, t_{n}) - y_{vv}(v, t_{n}) \right] = q(v, t_{n+1})$$
(13)

Discretizing (13) for  $\theta = 1$ , we get

$$(\ell + \phi_0 + \psi) y_r^{n+1} - (2\ell + \phi_0) y_r^n + \ell y_r^{n-1} + \ell \sum_{r=1}^n k_s [y_r^{n-s+1} - 2y_r^{n-s} + y_r^{n-s-1}] - (y_{vv})_r^{n+1} = q_r^{n+1}, \quad n = 0, 1, ..., N$$
(14)

Where  $\ell = \frac{\mu R(\alpha)}{\alpha (\Delta t)^2}$ ,  $\phi_0 = \frac{\phi}{\Delta t}$ ,  $y_r^n = y(v_r, t_n)$  and  $q_r^{n+1} = q(v_r, t_{n+1})$ . It has been found that the term  $y^{-1}$ 

occurs when n = s or n = 0. To get rid of  $y^{-1}$ , after solving this  $y^0 = \frac{v^1 - v^{-1}}{2\Delta t}$ , we use initial condition to get

$$y^{-1} = y^{1} - 2\Delta t \omega_{2}(v). \tag{15}$$

When we use the HCBS estimate and its essential derivatives at node  $v_r$  in Eq (14), then

$$(\ell + \phi_0 + \psi)Y_r^{n+1} - (Y_{yy})_r^{n+1}$$

$$= (2\ell + \phi_0)Y_r^n - \ell Y_r^{n-1} - \ell \sum_{s=1}^n k_s [Y_r^{n-s+1} - 2Y_r^{n-s} + Y_r^{n-s-1}] + q_r^{n+1}$$
(16)

Substituting (8) in (16), we get

$$(\ell + \phi_0 + \psi) \left( \lambda_1 \mathcal{G}_{r-1}^{n+1} + \lambda_2 \mathcal{G}_r^{n+1} + \lambda_1 \mathcal{G}_{r+1}^{n+1} \right) - \left( \lambda_5 \mathcal{G}_{r-1}^{n+1} + \lambda_6 \mathcal{G}_r^{n+1} + \lambda_5 \mathcal{G}_{r+1}^{n+1} \right)$$

$$= (2\ell + \phi_0) \left( \lambda_1 \mathcal{G}_{r-1}^n + \lambda_2 \mathcal{G}_r^n + \lambda_1 \mathcal{G}_{r+1}^n \right) - \ell \left( \lambda_1 \mathcal{G}_{r-1}^{n-1} + \lambda_2 \mathcal{G}_r^{n-1} + \lambda_1 \mathcal{G}_{r+1}^{n-1} \right)$$
(17)

$$-\ell \sum_{s=1}^{n} k_{s} \left[ \lambda_{1} \mathcal{G}_{r-1}^{n-s+1} + \lambda_{2} \mathcal{G}_{r}^{n-s+1} + \lambda_{1} \mathcal{G}_{r+1}^{n-s+1} - 2 \left( \lambda_{1} \mathcal{G}_{r-1}^{n-s} + \lambda_{2} \mathcal{G}_{r}^{n-s} + \lambda_{1} \mathcal{G}_{r+1}^{n-s} \right) + \lambda_{1} \mathcal{G}_{r-1}^{n-s-1} + \lambda_{2} \mathcal{G}_{r}^{n-s-1} + \lambda_{1} \mathcal{G}_{r+1}^{n-s-1} \right] + q_{r}^{n+1}$$

$$\left[ (\ell + \phi_{0} + \psi) \lambda_{1} - \lambda_{5} \right] \mathcal{G}_{r-1}^{n+1} + \left[ (\ell + \phi_{0} + \psi) \lambda_{2} - \lambda_{6} \right] \mathcal{G}_{r}^{n+1} + \left[ (\ell + \phi_{0} + \psi) \lambda_{1} - \lambda_{5} \right] \mathcal{G}_{r+1}^{n+1}$$

$$= (2\ell + \phi_{0}) \left[ \lambda_{1} \mathcal{G}_{r-1}^{n} + \lambda_{2} \mathcal{G}_{r}^{n} + \lambda_{1} \mathcal{G}_{r+1}^{n} \right] - \ell \left( \lambda_{1} \mathcal{G}_{r-1}^{n-1} + \lambda_{2} \mathcal{G}_{r}^{n-1} + \lambda_{1} \mathcal{G}_{r+1}^{n-1} \right)$$

$$-\ell \sum_{s=1}^{n} k_{s} \left[ \lambda_{1} \mathcal{G}_{r-1}^{n-s+1} + \lambda_{2} \mathcal{G}_{r}^{n-s+1} + \lambda_{1} \mathcal{G}_{r+1}^{n-s+1} - 2 \left( \lambda_{1} \mathcal{G}_{r-1}^{n-s} + \lambda_{2} \mathcal{G}_{r}^{n-s} + \lambda_{1} \mathcal{G}_{r+1}^{n-s} \right) + \lambda_{1} \mathcal{G}_{r-1}^{n-s} + \lambda_{2} \mathcal{G}_{r}^{n-s-1} + \lambda_{1} \mathcal{G}_{r+1}^{n-s-1} \right] + q_{r}^{n+1}$$

$$\left[ (\ell + \phi_{0} + \psi) \lambda_{1} - \lambda_{5} \right] \mathcal{G}_{r-1}^{n+1} + \left[ (\ell + \phi_{0} + \psi) \lambda_{2} - \lambda_{6} \right] \mathcal{G}_{r}^{n+1} + \left[ (\ell + \phi_{0} + \psi) \lambda_{1} - \lambda_{5} \right] \mathcal{G}_{r+1}^{n+1} \right] - \ell \left( \lambda_{1} \mathcal{G}_{r-1}^{n-1} + \lambda_{2} \mathcal{G}_{r}^{n-1} + \lambda_{1} \mathcal{G}_{r+1}^{n-1} \right)$$

$$-\ell \sum_{s=1}^{n} k_{s} \left[ \lambda_{1} (\mathcal{G}_{r-1}^{n-s+1} - 2 \mathcal{G}_{r-1}^{n-s} + \mathcal{G}_{r-1}^{n-s-1}) + \lambda_{2} (\mathcal{G}_{r}^{n-s+1} - 2 \mathcal{G}_{r}^{n-s+1} - 2 \mathcal{G}_{r}^{n-s} + \mathcal{G}_{r}^{n-s-1} \right)$$

$$-\ell \sum_{s=1}^{n} k_{s} \left[ \lambda_{1} (\mathcal{G}_{r-1}^{n-s+1} - 2 \mathcal{G}_{r-1}^{n-s} + \mathcal{G}_{r-1}^{n-s-1}) + \lambda_{2} (\mathcal{G}_{r}^{n-s+1} - 2 \mathcal{G}_{r}^{n-s+1} - 2 \mathcal{G}_{r}^{n-s-1} + \lambda_{1} \mathcal{G}_{r-1}^{n-1} \right)$$

The values of  $\lambda_1, \lambda_2, \lambda_5$  is given in (9). This system (19) is made up of N+1 linear equations and N+3 unknowns. The boundary conditions (3) are used to get two extra equations that are needed to make the system consistent. So, a matrix system with dimensions  $(N+3) \times (N+3)$  is created, and it can be solved in a single way using any suitable method. Before using (19), the initial vector  $\mathcal{G}^0 = [\mathcal{G}^0_{-1}, \mathcal{G}^0_0, ...., \mathcal{G}^0_{N+1}]^T$  is achieved through the ICs as

$$\begin{cases} (Y_v)_r^0 = \omega_1'(v_r), & r = 0, \\ (Y)_r^0 = \omega_1(v_r), & r = 0, 1, ...., N, \\ (Y_v)_r^0 = \omega_1'(v_r), & r = N, \end{cases}$$
(20)

This is the matrix representation of Equation (20):

$$T9^0 = D,$$
 (21)

Where

$$T = \begin{bmatrix} \lambda_3 & 0 & \lambda_4 \\ \lambda_1 & \lambda_2 & \lambda_1 \\ & \lambda_1 & \lambda_2 & \lambda_1 \\ & & \ddots & \ddots & \ddots \\ & & & \lambda_1 & \lambda_2 & \lambda_1 \\ & & & \ddots & \ddots & \ddots \\ & & & & \lambda_1 & \lambda_2 & \lambda_1 \\ & & & & \lambda_1 & \lambda_2 & \lambda_1 \\ & & & & \lambda_1 & \lambda_2 & \lambda_1 \\ & & & & \lambda_3 & 0 & \lambda_4 \end{bmatrix} \text{ and } D = \begin{bmatrix} \omega_1'(v_0) \\ \omega_1(v_0) \\ \omega_1(v_1) \\ \vdots \\ \vdots \\ \omega_1(v_{N-1}) \\ \omega_1(v_N) \\ \omega_1'(v_N) \end{bmatrix}$$

Eq (21) can be handled using any numerical approach for  $9^{\circ}$ .

# 4. The stability of the presented scheme

It is safe to say that the numerical method is steady if the error doesn't get bigger while the calculation is being done [40]. To examine the stability of the specified scheme, Fourier analysis is used. Let  $\zeta^n$  and  $\zeta^n$  are analytical and numerical representations of the expansion variables, respectively. The error  $\beta^n$  is shown

$$\beta_r^n = \tau_r^n - \tilde{\tau}_r^n$$
,  $r = 1, ..., N-1$ ,  $n = 0, 1, ..., M$ 

From Eq. (19) we obtain

$$\begin{split} & \left[ (\ell + \phi_{0} + \psi) \lambda_{1} - \lambda_{5} \right] \beta_{r-1}^{n+1} + \left[ (\ell + \phi_{0} + \psi) \lambda_{2} - \lambda_{6} \right] \beta_{r}^{n+1} + \left[ (\ell + \phi_{0} + \psi) \lambda_{1} - \lambda_{5} \right] \beta_{r+1}^{n+1} \\ &= (2\ell + \phi_{0}) \left[ \lambda_{1} \beta_{r-1}^{n} + \lambda_{2} \beta_{r}^{n} + \lambda_{1} \beta_{r+1}^{n} \right] - \ell \left( \lambda_{1} \beta_{r-1}^{n-1} + \lambda_{2} \beta_{r}^{n-1} + \lambda_{1} \beta_{r+1}^{n-1} \right) \\ &- \ell \sum_{s=1}^{n} k_{s} \left[ \lambda_{1} (\beta_{r-1}^{n-s+1} - 2\beta_{r-1}^{n-s} + \beta_{r-1}^{n-s-1}) + \lambda_{2} (\beta_{r}^{n-s+1} - 2\beta_{r}^{n-s} + \beta_{r}^{n-s-1}) \right. \end{split}$$

$$(22)$$

$$+ \lambda_{1} (\beta_{r+1}^{n-s+1} - 2\beta_{r+1}^{n-s} + \beta_{r+1}^{n-s-1}] + q_{r}^{n+1} \end{split}$$

From ICs and BCs, we can write

$$\beta_r^0 = \omega_1(v), \quad (\beta_r)_r^0 = \omega_2(v_r), \quad r = 1, 2, 3, ...., N$$
 (23)

And

$$\beta_0^n = \psi_1(t_n), \quad \beta_N^n = \psi_2(t_n), \quad n = 0, 1, ..., M$$
 (24)

The grid function is stated as:

$$\beta^{n} = \begin{cases} \beta_{r}^{n}, & v \in (v_{r} - \frac{h}{2}, u_{r} + \frac{h}{2}], \ r = 1, 2, ..., N - 1. \\ 0, & v \in [a, a + \frac{h}{2}] \ or \ v \in [b - \frac{h}{2}, b]. \end{cases}$$
 (25)

The  $\beta^{n}(v)$  in the Fourier mode can be presented as:

$$\beta^{n}(v) = \sum_{m=-\infty}^{\infty} \mu^{n}(m)e^{\frac{2\pi i m v}{b-a}},$$
(26)

Where

$$\mu^{n}(m) = \frac{1}{b-a} \int_{a}^{b} \beta^{n}(v) e^{\frac{-2\pi i m v}{b-a}} dv, \quad n = 0, 1, 2, ..., M \text{ and } \beta^{n} = [\beta_{1}^{n}, \beta_{2}^{n}, ...., \beta_{N-1}^{n}]^{T}$$
(27)

Implementing | | 2 norm, we attain

$$\begin{split} \left\| \beta^{n} \right\|_{2} &= \sqrt{\sum_{r=1}^{N-1} h \left| \beta_{r}^{n} \right|^{2}} \\ &= \left( \int_{a}^{a+\frac{h}{2}} \left| \beta^{n} \right|^{2} dv + \sum_{r=1}^{N-1} \int_{u_{r}-\frac{h}{2}}^{u_{r}+\frac{h}{2}} \left| \beta^{n} \right|^{2} dv + \int_{b-\frac{h}{2}}^{b} \left| \beta^{n} \right|^{2} dv \right)^{\frac{1}{2}} \\ &= \left( \int_{a}^{b} \left| \beta^{n} \right|^{2} dv \right)^{\frac{1}{2}} \end{split}$$

Using Perceval's identity (5), we achieve

$$\int_{a}^{b} \left| \beta^{n} \right|^{2} dv = \sum_{m=-\infty}^{\infty} \left| \mu^{n}(m) \right|^{2}$$

Hence we get

$$\|\beta^n\|_2^2 = \sum_{m=-\infty}^{\infty} |\mu^n(m)|^2$$
 (28)

Assume that the expressions (22)-(24) gives the solution in Fourier form as:

$$\beta_r^n = \mu^n e^{i\rho rh} \tag{29}$$

Where i and  $\sqrt{-1}$  is any real number. Substituting (29) in (22) and dividing by  $e^{iprh}$ 

$$\begin{split} & \left[ (\ell + \phi_0 + \psi) \lambda_1 - \lambda_5 \right] \mu^{n+1} e^{-i\rho h} + \left[ (\ell + \phi_0 + \psi) \lambda_2 - \lambda_6 \right] \mu^{n+1} + \left[ (\ell + \phi_0 + \psi) \lambda_1 - \lambda_5 \right] \mu^{n+1} e^{i\rho h} \\ &= (2\ell + \phi_0) \left[ \lambda_1 \mu^n e^{-i\rho h} + \lambda_2 \mu^n + \lambda_1 \mu^n e^{i\rho h} \right] - \ell \left( \lambda_1 \mu^{n-1} e^{-i\rho h} + \lambda_2 \mu^{n-1} + \lambda_1 \mu^{n-1} e^{i\rho h} \right) \\ &- \ell \sum_{s=1}^n k_s \left[ \lambda_1 (\mu^{n-s+1} e^{-i\rho h} - 2\mu^{n-s} e^{-i\rho h} + \mu^{n-s-1} e^{-i\rho h}) + \lambda_2 (\mu^{n-s+1} - 2\mu^{n-s} + \mu^{n-s-1}) \right. \end{split}$$
(30)  
 
$$+ \lambda_1 (\mu^{n-s+1} e^{i\rho h} - 2\mu^{n-s} e^{i\rho h} + \mu^{n-s-1} e^{i\rho h}) \end{split}$$

Utilizing the relation  $\cos(\rho h) = \frac{e^{i\rho h} + e^{-i\rho h}}{2}$  and simplifying, we get

$$\mu^{n+1} = \frac{(1+\Re)}{\sigma} \mu^n - \frac{\Re}{\sigma} \mu^{n-1} - \frac{\Re}{\sigma} \sum_{s=1}^n k_s (\mu^{n-s+1} - 2\mu^{n-s} + \mu^{n-s-1})$$
(31)

Where 
$$\Re = \frac{\ell}{\ell + \phi_0}$$
 and  $\sigma = 1 + \frac{2\cos(\rho h)(\psi h^2 - 6) + 4\psi h^2 + 12}{(\ell h^2 + \phi_0 h^2)(2\cos(\rho h) + 4)}$ . Obviously  $\sigma \ge 1$ 

# Lemma 4.1

If the answer to Eq. (31) is  $\mu^n$ , then  $|\mu^n| \le (1+\Re) |\mu^0|$ ,  $n = 0,1,\ldots,M$ .

Proof: We employed the induction method to prove this lemma. Put n = 0 in the Eq. (31)

$$\left|\mu^{1}\right| = \frac{(1+\Re)}{\sigma} \left|\mu^{0}\right| \leq (1+\Re) \left|\mu^{0}\right|, \quad \sigma \geq 1.$$

Assume that  $|\mu^n| \le (1+\Re) |\mu^0|$ , for n = 1, 2, ..., M-1. then

$$\begin{split} \left|\mu^{n+1}\right| &\leq \frac{(1+\Re)}{\sigma} \left|\mu^{n}\right| - \frac{\Re}{\sigma} \left|\mu^{n-1}\right| - \frac{\Re}{\sigma} \sum_{s=1}^{n} k_{s} \left[\left|\mu^{n-s+1}\right| - 2\left|\mu^{n-s}\right| + \left|\mu^{n-s-1}\right|\right], \\ &\leq \frac{(1+\Re)^{2}}{\sigma} \left|\mu^{0}\right| - \frac{\Re(1+\Re)}{\sigma} \left|\mu^{0}\right| - \frac{\Re(1+\Re)}{\sigma} \sum_{s=1}^{n} k_{s} \left[\left|\mu^{0}\right| - 2\left|\mu^{0}\right| + \left|\mu^{0}\right|\right], \\ &= \frac{(1+\Re)}{\sigma} \left[1 + \Re - \Re\right] \left|\mu^{0}\right|, \\ \left|\mu^{n+1}\right| &\leq (1+\Re) \left|\mu^{0}\right|. \end{split}$$

**Theorem 1.** The method presented in (19) is stable unconditionally.

Proof: By using Eq (28) and Proposition 4.1, we attain

$$\|\beta^n\|_2 \le (1+\Re) \|\beta^0\|_2$$
,  $n = 0,1,...,M$ .

As a result, the proposed computational approach is always and unconditionally stable.

# **5** Convergence

The convergence of the proposed method is examined using the technique described in [41]. The following theorem is first introduced as [40][41]

**Theorem 2** Let q is connected to  $C^2[a,b]$  and y(v,t) is associated to  $C^4[a,b]$  also subdivision of [a,b] is  $\Upsilon = \{a = v_0, v_1, ..., v_N = b\}$  with  $v_r = a + rh$ , r = 0,1,2,...,N. If the curve of the solution is connected by a single spline Y(v,t) at  $v_r \in \Upsilon$ , then for every  $t \geq 0$ , there is a number  $\zeta_r$  not related to h such that for r = 0, 1, 2, we get

$$||D^{r}(y(v,t) - \tilde{Y}(u,t))||_{x} \le \zeta_{r}h^{4-r}$$
 (32)

**Lemma 5.1** The HCBS set  $\{S_{-1}, S_0, \dots, S_{N-1}\}$  in (6) fulfils the inequality as given in [44]

$$\sum_{r=-1}^{N+1} \left| S_r(v) \right| \le \frac{5}{3}, \quad 0 \le v \le 1.$$
 (33)

**Theorem 3:** The numerical solution Y(v,t) exists for the exact solution y(v,t) concerning TFDWE

(1)-(3). Moreover, if q belongs to  $C^2$  [0, 1], then

$$||y(v,t) - Y(v,t)||_{\infty} \le \tilde{\zeta}h^2, \ \forall \ t \ge 0,$$
 (34)

Proof: Let  $\tilde{Y}(v,t) = \sum_{r=-1}^{N+1} x_r^n(t) S_r(v)$  be the estimated HCBS for Y(v,t). By applying the triangle

inequality, we obtain

$$||y(v,t) - Y(v,t)||_{\infty} \le ||y(v,t) - \tilde{Y}(v,t)||_{\infty} + ||\tilde{Y}(v,t) - Y(v,t)||_{\infty}$$

Utilizing Theorem 2 for r = 0, we achieve

$$\|y(v,t) - Y(v,t)\|_{\infty} \le \zeta_0 h^4 + \|\tilde{Y}(v,t) - Y(v,t)\|_{\infty}.$$
 (35)

There are collocation conditions in the current method.

$$Ly(v_r,t) = LY(v_r,t) = q(v_r,t), r = 0,1,...,N.$$
 Consider

$$L\tilde{Y}(v_r,t) = \tilde{q}(v_r,t).$$

Therefore, the difference equation  $L(\tilde{Y}(v_r,t)-Y(v_r,t))$  can be expressed at temporal level n as

$$\begin{split} & \left[ (\ell + \phi_{0} + \psi) \lambda_{1} - \lambda_{5} \right] \mathcal{O}_{r-1}^{n+1} + \left[ (\ell + \phi_{0} + \psi) \lambda_{2} - \lambda_{6} \right] \mathcal{O}_{r}^{n+1} + \left[ (\ell + \phi_{0} + \psi) \lambda_{1} - \lambda_{5} \right] \mathcal{O}_{r+1}^{n+1} \\ &= (2\ell + \phi_{0}) \left[ \lambda_{1} \mathcal{O}_{r-1}^{n} + \lambda_{2} \mathcal{O}_{r}^{n} + \lambda_{1} \mathcal{O}_{r+1}^{n} \right] - \ell \left( \lambda_{1} \mathcal{O}_{r-1}^{n-1} + \lambda_{2} \mathcal{O}_{r}^{n-1} + \lambda_{1} \mathcal{O}_{r+1}^{n-1} \right) \\ &- \ell \sum_{s=1}^{n} k_{s} \left[ \lambda_{1} (\mathcal{O}_{r-1}^{n-s+1} - 2\mathcal{O}_{r-1}^{n-s} + \mathcal{O}_{r-1}^{n-s-1}) + \lambda_{2} (\mathcal{O}_{r}^{n-s+1} - 2\mathcal{O}_{r}^{n-s} + \mathcal{O}_{r}^{n-s-1}) \right. \\ &+ \lambda_{1} (\mathcal{O}_{r+1}^{n-s+1} - 2\mathcal{O}_{r+1}^{n-s} + \mathcal{O}_{r+1}^{n-s-1}) + \frac{1}{h^{2}} \zeta_{r}^{n+1} \end{split}$$

The BCs can be given as

$$\lambda_1 \mathcal{O}_{r-1}^{n+1} + \lambda_2 \mathcal{O}_r^{n+1} + \lambda_1 \mathcal{O}_{r+1}^{n+1} = 0, \quad r = 0, N$$

Where

$$\mathfrak{O}_r^n = \mathfrak{S}_r^n - x_r^n, \quad r = -1, 0, ..., N+1$$

and

$$\varsigma_r^n = h^2 [q_r^n - \tilde{q}_r^n], \quad r = 0, 1, ..., N$$

From inequality (29), we achieve

$$\left|\varsigma_r^n\right| = h^2 [q_r^n - \tilde{q}_r^n] \le \zeta h^4.$$

Define  $\zeta^n = \max_{0 \le r \le N} |\zeta_r^n|, e_r^n = |\mathfrak{T}_r^n|$  and  $e^n = \max_{0 \le r \le N} |e_r^n|$ . When n = 0 and using the equation (15),

Equation (36) transforms into

$$\begin{split} & \left[ \lambda_1 (\phi_0 + \psi) - \lambda_5 \right] \boldsymbol{\nabla}_{r-1}^1 + \left[ \lambda_2 (\phi_0 + \psi) - \lambda_6 \right] \boldsymbol{\nabla}_r^1 + \left[ \lambda_1 (\phi_0 + \psi) - \lambda_5 \right] \boldsymbol{\nabla}_{r+1}^1 \\ &= \phi_0 \left( \lambda_1 \boldsymbol{\nabla}_{r-1}^0 + \lambda_2 \boldsymbol{\nabla}_r^0 + \lambda_1 \boldsymbol{\nabla}_{r+1}^0 \right) + \frac{1}{h^2} \boldsymbol{\zeta}_r^1 \end{split}$$

Where r = 0, 1, ..., N. Using IC,  $e^0 = 0$ 

$$\left[\lambda_{2}(\phi_{0}+\psi)-\lambda_{6}\right] \mathcal{O}_{r}^{1} = -\left[\lambda_{1}(\phi_{0}+\psi)-\lambda_{5}\right] \left(\mathcal{O}_{r-1}^{1}+\mathcal{O}_{r+1}^{1}\right) + \frac{1}{h^{2}} \zeta_{r}^{1}$$

Taking the magnitude of  $\mathfrak{F}_r^1, \zeta_r^1$  and small value of h, So

$$e_r^1 \le \frac{3\zeta h^4}{h^2(\phi_0 + \psi) + 12}, \quad 0 \le r \le N.$$

BCs provide the values of  $e_{-1}^1$  and  $e_{N+1}^1$ :

$$e_{-1}^{1} \le \frac{15\zeta h^{4}}{h^{2}(\phi_{0} + \psi) + 12},$$
 $e_{N+1}^{1} \le \frac{15\zeta h^{4}}{h^{2}(\phi_{0} + \psi) + 12},$ 
Which implies
 $e^{1} \le \zeta_{1}h^{2},$ 

Where  $\zeta_1$  is independent of h. Now, this theorem is proved via mathematical induction. Suppose that  $e_r^u \le \zeta_u h^2$  is true for  $1 \le u \le n$  and  $\zeta = \max\{\zeta_u : u = 0, 1, ..., n\}$ . subsequently, using Equation (33), we obtain

$$\begin{split} & \left[ \lambda_{1} (\ell + \phi_{0} + \psi) - \lambda_{4} \right] \boldsymbol{\nabla}_{r-1}^{n+1} + \left[ \lambda_{2} (\ell + \phi_{0} + \psi) + 2 \lambda_{4} \right] \boldsymbol{\nabla}_{r}^{n+1} + \left[ \lambda_{1} (\ell + \phi_{0} + \psi) - \lambda_{4} \right] \boldsymbol{\nabla}_{r+1}^{n+1} \\ &= (2\ell + \phi_{0} - \ell k_{1}) \left( \lambda_{1} \boldsymbol{\nabla}_{r-1}^{n} + \lambda_{2} \boldsymbol{\nabla}_{r}^{n} + \lambda_{1} \boldsymbol{\nabla}_{r+1}^{n} \right) - \ell \left[ (k_{0} - 2k_{1} + k_{2}) \right] \left( \lambda_{1} \boldsymbol{\nabla}_{r-1}^{n-1} + \lambda_{2} \boldsymbol{\nabla}_{r}^{n-1} + \lambda_{1} \boldsymbol{\nabla}_{r+1}^{n-1} \right) \\ &+ (k_{1} - 2k_{2} + k_{3}) \left( \lambda_{1} \boldsymbol{\nabla}_{r-1}^{n-2} + \lambda_{2} \boldsymbol{\nabla}_{r}^{n-2} + \lambda_{1} \boldsymbol{\nabla}_{r+1}^{n-2} \right) + (k_{2} - 2k_{3} + k_{4}) \left( \lambda_{1} \boldsymbol{\nabla}_{r-1}^{n-3} + \lambda_{2} \boldsymbol{\nabla}_{r}^{n-3} + \lambda_{1} \boldsymbol{\nabla}_{r+1}^{n-3} \right) + \\ &\dots + (k_{n-3} - 2k_{n-2} + k_{n-1}) \left( \lambda_{1} \boldsymbol{\nabla}_{r-1}^{2} + \lambda_{2} \boldsymbol{\nabla}_{r}^{2} + \lambda_{1} \boldsymbol{\nabla}_{r+1}^{2} \right) + (k_{n-2} - 2k_{n-1} + k_{n}) \left( \lambda_{1} \boldsymbol{\nabla}_{r-1}^{1} + \lambda_{2} \boldsymbol{\nabla}_{r}^{1} + \lambda_{1} \boldsymbol{\nabla}_{r+1}^{1} \right) \\ &+ k_{n-1} \left( \lambda_{1} \boldsymbol{\nabla}_{r-1}^{0} + \lambda_{2} \boldsymbol{\nabla}_{r}^{0} + \lambda_{1} \boldsymbol{\nabla}_{r+1}^{0} \right) - k_{n} \left( \lambda_{1} \boldsymbol{\nabla}_{r-1}^{1} + \lambda_{2} \boldsymbol{\nabla}_{r}^{1} + \lambda_{1} \boldsymbol{\nabla}_{r+1}^{1} \right) \right] + \frac{1}{h^{2}} \boldsymbol{\varsigma}_{r}^{n+1}. \end{split}$$

Again, taking the modulus of  $\mathfrak{T}_r^{n+1}$  and  $\zeta_r^{n+1}$ , we get

$$e_r^{n+1} \leq \frac{3h^2}{h^2(\ell+\phi_0+\psi)+12} \left[ (2\ell+\phi_0-\ell k_1)\zeta h^2 - \ell \sum_{s=1}^{n-1} (k_{s-1}-2k_s+k_{s+1})\zeta h^2 + \ell k_n \zeta h^2 + \zeta h^2 \right].$$

Similarly, after applying the BCs, we get the values of  $e_{-1}^{n+1}$  and  $e_{N+1}^{n+1}$ 

$$e_{-1}^{n+1} \leq \frac{15h^2}{h^2(\ell+\phi_0+\psi)+12} \left[ (2\ell+\phi_0-\ell k_1)\zeta h^2 - \ell \sum_{s=1}^{n-1} (k_{s-1}-2k_s+k_{s+1})\zeta h^2 + \ell k_n \zeta h^2 + \zeta h^2 \right].$$

And

$$e_{N+1}^{n+1} \leq \frac{15h^2}{h^2(\ell+\phi_0+\psi)+12} \left[ (2\ell+\phi_0-\ell k_1)\zeta h^2 - \ell \sum_{s=1}^{n-1} (k_{s-1}-2k_s+k_{s+1})\zeta h^2 + \ell k_n \zeta h^2 + \zeta h^2 \right].$$

Hence, for all n, we acquire

$$e^{n+1} \le \zeta h^2. \tag{37}$$

In particular,

$$\tilde{Y}(v,t) - Y(v,t) = \sum_{r=-1}^{N+1} (x_r(t) - \theta_r(t)S_r(v).$$
(38)

Therefore, from Lemma 5.1 and inequality (37), we get

$$\|\ddot{Y}(v,t) - Y(v,t)\|_{\infty} \le \frac{5}{3}\zeta h^2$$
 (39)

Using (38), the inequality (35) becomes

$$||y(v,t)-Y(v,t)||_{\infty} \le \zeta h^4 + \frac{5}{3} \zeta h^2 = \tilde{\zeta} h^2,$$

Where

$$\tilde{\zeta} = \zeta_0 h^2 + \frac{5}{3} \zeta.$$

**Theorem 4** The TFDWE converges with initial conditions and boundary conditions.

Proof. Let us consider the numerical and estimated results for TFDWE are y(v, t) and Y(v, t), respectively. Consequently, the previously mentioned theory and relation (12) verify the presence of constants  $\zeta$  and F and F such that

$$||y(v,t)-Y(v,t)||_{\infty} \leq \zeta h^2 + F(\Delta t)^2.$$

Consequently, the suggested technique exhibits quadratic convergence.

# 6. Numerical Experiments

Numerical results from trials by utilizing the suggested method are shown in this section. We use the error norms  $L_2$  and  $L_{\infty}$  as a means of evaluating the accuracy of the proposed method as in [45].

$$L_{\infty} = \|y(v_r, t) - Y(v_r, t)\|_{\infty} = \max_{0 \le r \le N} |y(v_r, t) - Y(v_r, t)|$$

And

$$L_2 = \left\| y(v_r, t) - Y(v_r, t) \right\|_2 = \sqrt{h \sum_{r=0}^{N} \left| y(v_r, t) - Y(v_r, t) \right|^2} \ .$$

Moreover, the Experimental order of convergence (EOC) is computed as in [46]

$$EOC = \frac{\log\left(\frac{L_{\infty}(n)}{L_{\infty}(2n)}\right)}{\log(2)}$$

By doing so  $R(\alpha) = 1$ , Mathematica 12 is used to perform numerical computations on an Intel(R) Core (TM) i5-3437U CPU running at 1.90GHz and 2.40GHz with 12.0 GB of RAM, an SSD, and a 64-bit operating system (Windows 10).

# Example 6.1

$$\frac{\partial^{\alpha}}{\partial t^{\alpha}} y(v,t) = \frac{\partial^{2}}{\partial v^{2}} y(v,t) + q(v,t), \quad (v,t) \in [0,1] \times [0,T].$$

$$y(v,0) = 0, \quad y_{t}(v,0) = -\sin(\pi v),$$

$$v(0,t) = v(1,t) = 0.$$
(40)

Where the source term is  $q(v,t) = \frac{2t^{2-\alpha}\sin(\pi v)}{\Gamma(3-\alpha)} + (t^2-t)\sin(\pi v)\pi^2$ . The exact solution to the given problem is  $y(v,t) = \sin(\pi v)(t^2-t)$  [22].

Table 1: Comparison of maximum error at different values of h,  $\Delta t$  when  $\alpha = 1.5$  and t = 0.2 for example 1

h	$\Delta t$	HF [22]	$\alpha = 1.5$	<b>Present Method</b>
0.2	0.02	0.01149	6.410×10 <sup>-4</sup>	3.2191×10 <sup>-6</sup>
0.1	0.01	0.00361	8.203×10 <sup>-5</sup>	6.4073×10 <sup>-7</sup>
0.05	0.006	0.00120	1.027×10 <sup>-5</sup>	2.3318×10 <sup>-7</sup>
0.03	0.006	0.00115	3.049×10 <sup>-6</sup>	9.4654×10 <sup>-8</sup>
0.03	0.005	0.00021	3.035×10 <sup>-6</sup>	5.3228×10 <sup>-8</sup>
0.025	0.005	0.00019	1.281×10 <sup>-6</sup>	3.0147×10 <sup>-8</sup>
0.025	0.0047	0.00006	1.280×10 <sup>-6</sup>	8.8916×10 <sup>-9</sup>
0.02	0.0045	0.00004	8.989×10 <sup>-7</sup>	4.3751×10 <sup>-9</sup>

The findings are given for  $\alpha=1.5$  and t=0.2 in Table 1. The results demonstrate that the maximum error related to the suggested approach dramatically drops as the mesh is fine-tuned, or as h and  $\Delta t$  decrease. For example, when h=0.02 and  $\Delta t=0.0045$ , the suggested approach obtains the maximum error of the order  $10^{-9}$ , which is less than the error in [22] and [36]. This implies that even with minor grid improvements, the proposed strategy improves accuracy.

Table 2: The maximum error at different values of h,  $\Delta t$  when  $\alpha = 1.7$  and t = 0.4 for example 1.

h	Δt	HF [22]	CuTBSM [36]	<b>Present Method</b>
0.1	0.02	0.01396	2.490×10 <sup>-4</sup>	4.0376×10 <sup>-6</sup>
0.05	0.01	0.01064	3.113×10 <sup>-5</sup>	5.2260×10 <sup>-7</sup>
0.03	0.005	0.00736	9.178×10 <sup>-6</sup>	8.3124×10 <sup>-8</sup>
0.02	0.004	0.00653	1.982×10 <sup>-6</sup>	6.0035×10 <sup>-8</sup>
0.02	0.003	0.00586	1.980×10 <sup>-6</sup>	5.9821×10 <sup>-8</sup>
0.01	0.0025	0.00494	1.149×10 <sup>-6</sup>	3.4888×10 <sup>-9</sup>
0.01	0.0022	0.00460	1.443×10 <sup>-6</sup>	6.0094×10 <sup>-10</sup>
0.014	0.0020	0.00443	7.202×10 <sup>-7</sup>	4.8107×10 <sup>-10</sup>

Table 3: Example 1's error norms and order of convergence for various N when

$$\Delta t = \frac{1}{120}, \alpha = 1.5$$

N	L <sub>2</sub> Norm	$L_{\infty}$ Norm	EOC
10	2.9355×10 <sup>-4</sup>	3.1950×10 <sup>-4</sup>	
20	8.7109×10 <sup>-5</sup>	9.0451×10 <sup>-5</sup>	1.8681
40	2.2128×10 <sup>-5</sup>	2.4778×10 <sup>-5</sup>	1.3654
80	5.9376×10 <sup>-6</sup>	9.7562×10 <sup>-6</sup>	1.9777

In Table 2, when we increased the  $\alpha$  at time t = 0.4 the maximum error began to decrease with finer grids. The maximum error of order  $10^{-10}$  which is smaller than mentioned methods.

In Table 3,  $L_2$  and  $L_\infty$  error norms along with the observed spatial order of convergence are discussed, for Example 1 when N is increased gradually and the time step size  $\Delta t = \frac{1}{120}$  is fixed.

The fractional order is taken as  $\alpha = 1.5$ . The table shows that mesh refinement enhances scheme correctness by decreasing both error norms as N increases. Moreover, as N rises, the anticipated order of convergence gets closer to 2. As an example, the calculated order is around between and stays extremely close to 2 in further revisions.

Table 4: Error norms when  $\Delta t = \frac{1}{120}$ ,  $\alpha = 1.5$ ,  $h = \frac{1}{60}$  at different time levels for Example 1.

t	L <sub>2</sub> Norm	L <sub>∞</sub> Norm
0.2	$4.3007 \times 10^{-9}$	7.4631×10 <sup>-9</sup>
0.4	5.9111×10 <sup>-8</sup>	$8.2947 \times 10^{-8}$
1.0	2.4189×10 <sup>-8</sup>	4.0933×10 <sup>-8</sup>
2.0	3.6484×10 <sup>-7</sup>	5.2149×10 <sup>-7</sup>

Similarly, in Table 4 L<sub>2</sub> and L<sub> $\infty$ </sub> are discussed with different time levels when the spatial step size  $h = \frac{1}{60}$ 

, time step  $\Delta t = \frac{1}{120}$  and  $\alpha = 1.5$ . This table shows as t increases, both error norms started increasing. Because fractional derivatives include memory effects, this gradual increase in inaccuracy over time is common in fractional differential equations. However, the error remains within reasonable bounds, indicating that the system maintains precision and stability across long simulation durations.

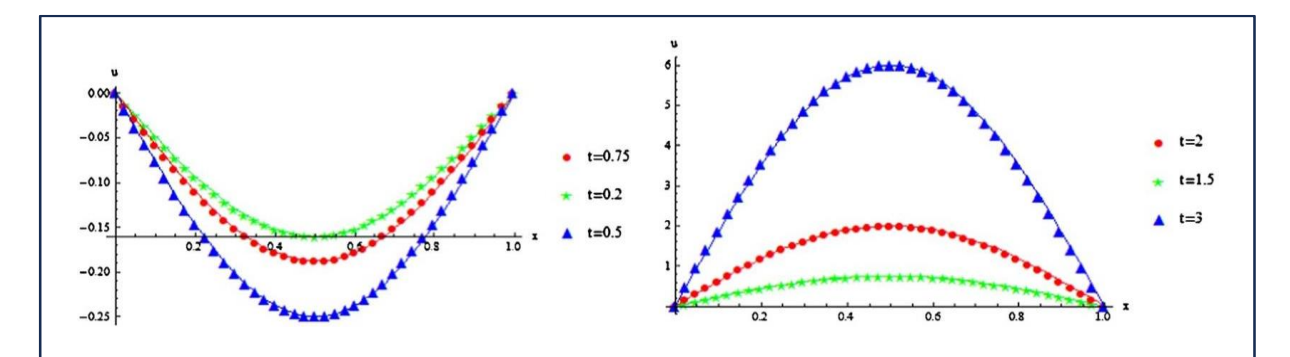
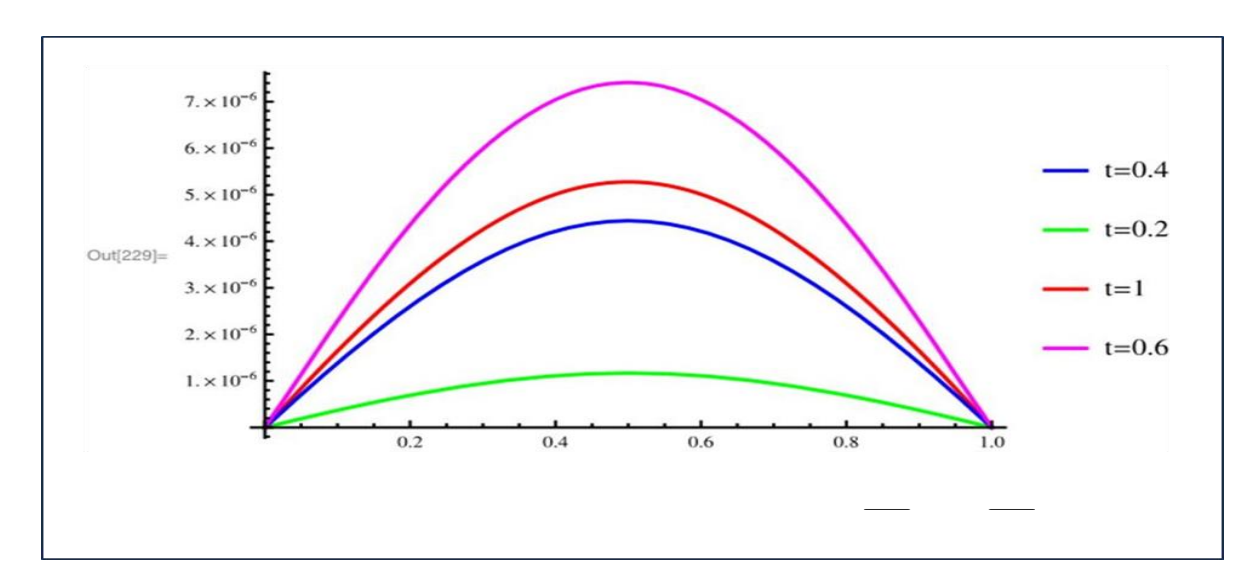


Figure 1: Numerical (stars, bullets) and exact solutions (solid lines) at various time levels when  $h=\frac{1}{80},\ t=\frac{1}{100}$  and  $\alpha=1.75$  for Example 1.



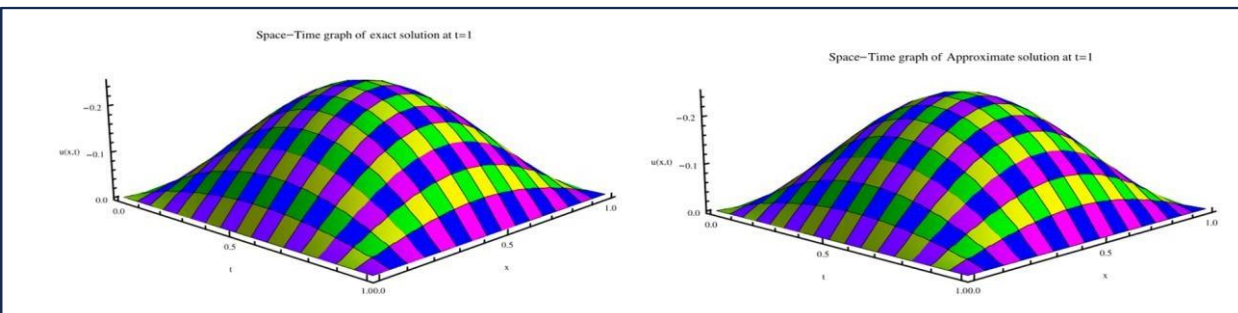


Figure 3: Three-dimensional comparison of exact (left) and numerical (right) solutions with  $h=\frac{1}{64}, \Delta t=\frac{1}{100}$  and  $\alpha=1.5$  at t=1 of Example 1.

Figure 1 displays the graphs of the exact and approximate solutions for a range of values of  $\alpha$ , h and t over different time periods. Excellent coordination among the solutions is displayed in the graphs. Figure 2 illustrates the absolute error trends at several time points, highlighting the method's great accuracy. It has been observed that our approach achieves much higher accuracy. The three-dimensional graphs of the exact and estimated solutions at time t=0.1 are contrasted in Figure 3.

# Example 2

$$\frac{\partial^{\alpha}}{\partial t^{\alpha}} y(v,t) + y(v,t) = \frac{\partial^{2}}{\partial v^{2}} y(v,t) + q(v,t), \quad (v,t) \in [0,1] \times [0,T].$$

$$y(v,0) = 0, \qquad y_{t}(v,0) = 0,$$

$$y(0,t) = y(1,t) = 0,$$
(41)

Where the source term is  $q(v,t) = \frac{2t^{2-\alpha}v(1-v)}{\Gamma(3-\alpha)} + t^2v(1-v) + 2t^2$ . The exact solution of given problem is  $y(v,t) = t^2v(1-v)$ .

The suggested approach is used to tackle this issue. Table 5-6 shows the absolute errors at various points  $v_i \in [0,1]$  for values  $\alpha$  chosen from the range  $1 < \alpha \le 2$ . At different time levels with  $\alpha = 1.5$ ,  $\Delta t = 0.01$  and t = 1 for N = 80. The findings demonstrate the method's stability and dependability by showing that the absolute error stays consistently low across all tested values of.

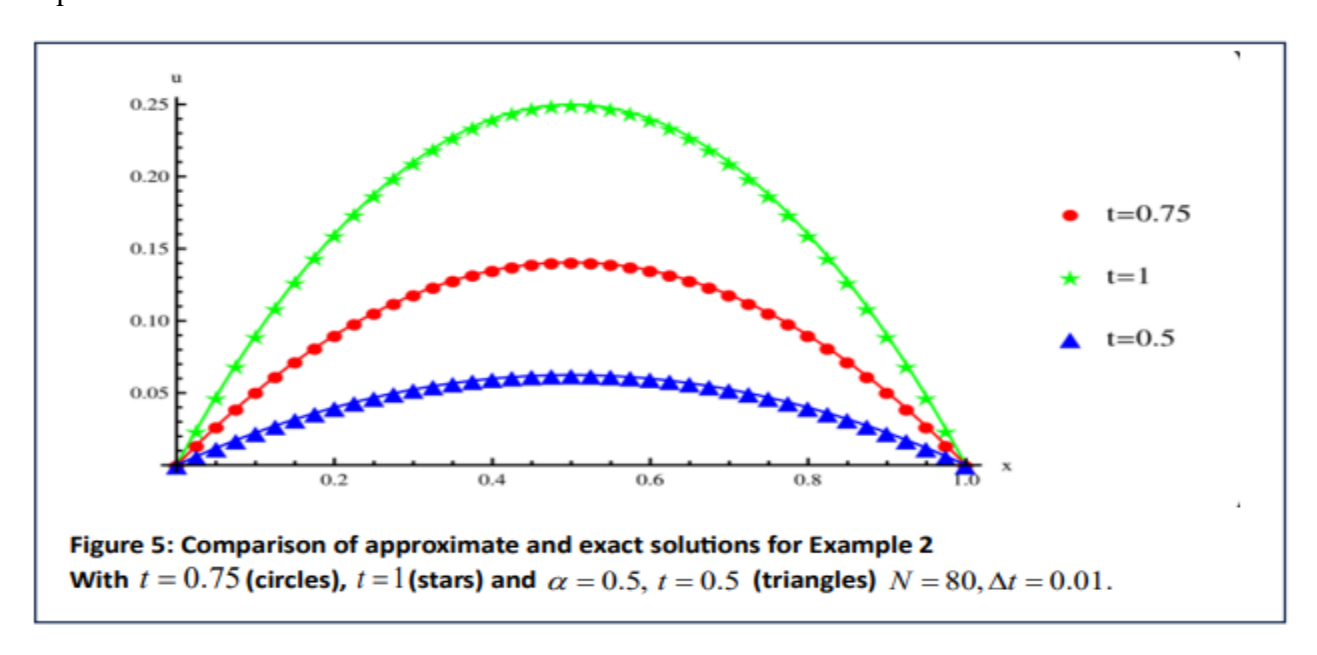
Table 5: Absolute error for different values of  $\alpha$ ,  $\nu$  with  $\Delta t = 0.01$  of Example 2.

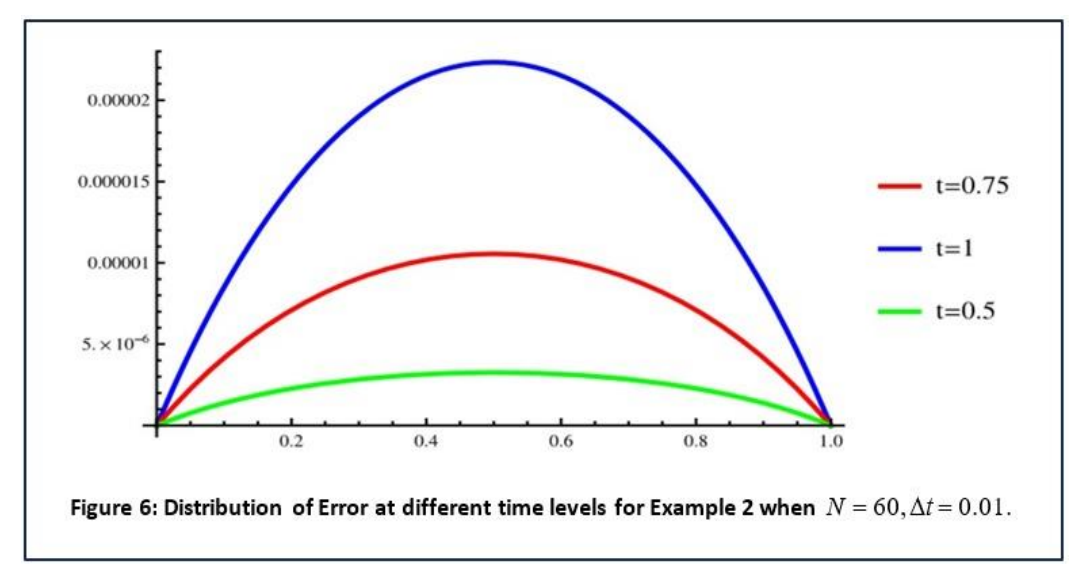
v	$\alpha = 1.1$	$\alpha = 1.3$	$\alpha = 1.5$	$\alpha = 1.7$	$\alpha = 1.9$
0	2.73045×10 <sup>-15</sup>	3.05311×10 <sup>-16</sup>	$7.56339 \times 10^{-16}$	2.03327×10 <sup>-14</sup>	6.245×10 <sup>-15</sup>
0.1	1.31839×10 <sup>-14</sup>	1.34059×10 <sup>-14</sup>	1.56403×10 <sup>-14</sup>	3.26128×10 <sup>-14</sup>	5.20695×10 <sup>-14</sup>
0.2	2.45082×10 <sup>-14</sup>	2.39253×10 <sup>-14</sup>	2.39808×10 <sup>-14</sup>	2.52298×10 <sup>-14</sup>	2.47025×10 <sup>-15</sup>
0.3	3.21687×10 <sup>-14</sup>	3.11695×10 <sup>-14</sup>	3.02258×10 <sup>-14</sup>	3.32234×10 <sup>-14</sup>	2.96985×10 <sup>-15</sup>
0.4	3.64986×10 <sup>-14</sup>	3.53328×10 <sup>-14</sup>	3.40006×10 <sup>-14</sup>	3.71092×10 <sup>-14</sup>	9.24261×10 <sup>-15</sup>
0.5	3.78586×10 <sup>-14</sup>	3.66929×10 <sup>-14</sup>	3.51941×10 <sup>-14</sup>	3.64153×10 <sup>-14</sup>	2.20934×10 <sup>-14</sup>
0.6	3.63598×10 <sup>-14</sup>	3.52218×10 <sup>-14</sup>	3.40283×10 <sup>-14</sup>	3.475×10 <sup>-14</sup>	2.13163×10 <sup>-14</sup>
0.7	3.21132×10 <sup>-14</sup>	3.11695×10 <sup>-14</sup>	3.00593×10 <sup>-14</sup>	$3.08364 \times 10^{-14}$	1.91236×10 <sup>-14</sup>
0.8	2.48135×10 <sup>-14</sup>	2.41196×10 <sup>-14</sup>	2.33147×10 <sup>-14</sup>	2.41196×10 <sup>-14</sup>	1.70697×10 <sup>-14</sup>
0.9	1.42525×10 <sup>-14</sup>	1.38917×10 <sup>-14</sup>	1.34476×10 <sup>-14</sup>	1.41553×10 <sup>-14</sup>	1.01863×10 <sup>-14</sup>
1	3.46945×10 <sup>-18</sup>	0	3.46945×10 <sup>-18</sup>	3.46945×10 <sup>-18</sup>	0

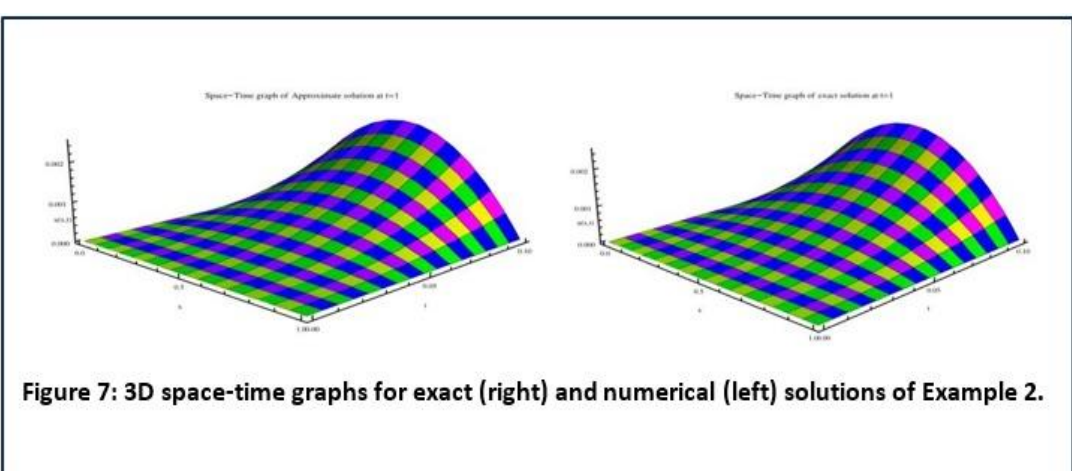
Table 6: Absolute error for different values of  $\alpha$ ,  $\nu$  with  $\Delta t = 0.1$  of Example 2.

v	$\alpha = 1.1$	$\alpha = 1.3$	$\alpha = 1.5$	$\alpha = 1.7$	$\alpha = 1.9$
0	4.59702×10 <sup>-16</sup>	2.54657×10 <sup>-15</sup>	$2.15626 \times 10^{-15}$	5.75581×10 <sup>-15</sup>	1.71738×10 <sup>-15</sup>
0.1	2.88078×10 <sup>-9</sup>	2.82613×10 <sup>-9</sup>	2.7629×10 <sup>-9</sup>	2.681×10 <sup>-9</sup>	2.57447×10 <sup>-9</sup>
0.2	5.02135×10 <sup>-9</sup>	4.91777×10 <sup>-9</sup>	4.79769×10 <sup>-9</sup>	4.64184×10 <sup>-9</sup>	4.43884×10 <sup>-9</sup>
0.3	6.4977×10 <sup>-9</sup>	$6.35567 \times 10^{-9}$	6.19068×10 <sup>-9</sup>	5.97609×10 <sup>-9</sup>	5.69615×10 <sup>-9</sup>
0.4	7.36274×10 <sup>-9</sup>	7.19622×10 <sup>-9</sup>	7.00249×10 <sup>-9</sup>	6.75017×10 <sup>-9</sup>	6.42064×10 <sup>-9</sup>
0.5	7.64765×10 <sup>-9</sup>	7.42273×10 <sup>-9</sup>	7.26912×10 <sup>-9</sup>	7.0038×10 <sup>-9</sup>	6.65713×10 <sup>-9</sup>
0.6	7.36274×10 <sup>-9</sup>	7.19622×10 <sup>-9</sup>	$7.00249 \times 10^{-9}$	6.75017×10 <sup>-9</sup>	6.42064×10 <sup>-9</sup>
0.7	6.4977×10 <sup>-9</sup>	$6.35567 \times 10^{-9}$	6.19068×10 <sup>-9</sup>	5.97609×10 <sup>-9</sup>	5.69615×10 <sup>-9</sup>
0.8	5.02135×10 <sup>-9</sup>	4.91777×10 <sup>-9</sup>	4.79769×10 <sup>-9</sup>	4.64184×10 <sup>-9</sup>	4.43884×10 <sup>-9</sup>
0.9	2.88078×10 <sup>-9</sup>	2.82613×10 <sup>-9</sup>	2.7629×10 <sup>-9</sup>	2.68099×10 <sup>-9</sup>	2.57447×10 <sup>-9</sup>
1	$6.93889 \times 10^{-18}$	3.46945×10 <sup>-18</sup>	6.93889×10 <sup>-16</sup>	3.46945×10 <sup>-18</sup>	0

Figure 5 shows the graphs of the exact and approximate solutions. A great degree of agreement exists between the exact and approximate solutions. Figure 6 ( $N = 60, \Delta t = 0.01$ ) plots the absolute error profile at various time levels to demonstrate the scheme's accuracy. By establishing the values of various parameters, Figure 7 displays the 3D plot of the estimated and exact solutions. There are a lot of similarities between the solutions. It is evident from Figure 7 and Table 5-6 that the suggested approach is highly precise and effective. For many values of  $\alpha$ , it is important to observe that the numerical solutions link quite well with the exact solutions.







# 7. Conclusion

This study dealt with the challenge of identifying approximate results to time-dependent fractional partial differential equations (FPDE). B-splines were employed to formulate a collocation approach for TFDWE to accomplish this objective. The spatial derivative was discretized using Hybrid Cubic B-splines, and the time fractional derivative was approximated using standard FDM.

Analyzing the approximated solutions of TFDWE, an efficient numerical approach that takes reaction and damping components into account has been presented. Together with CFFD, we have used the  $\theta$ -weighted approach and HCBS functions. The proposed technique shows quadratic temporal and spatial convergence and is unconditionally stable. We have looked at two numerical issues. The suggested approach is both accurate and computationally effective, as seen by the comparison of the numbers and graphics. We might investigate higher-dimensional and variable- order fractional partial differential equations in the future for numerical solutions by Hybrid-based Spline functions.

### REFERENCES

- [1] B. Ross, "Fractional calculus," Math. Mag., vol. 50, no. 3, pp. 115–122, 1977.
- [2] I. Podlubny, Fractional differential equations: an introduction to fractional derivatives, fractional differential equations, to methods of their solution and some of their applications. elsevier, 1998.
- [3] R. Hilfer, Applications of fractional calculus in physics. World scientific, 2000.
- [4] K. Diethelm and A. D. Freed, "On the solution of nonlinear fractional-order differential equations used in the modeling of viscoplasticity," in Scientific computing in chemical engineering II: computational fluid dynamics, reaction engineering, and molecular properties, Springer, 1999, pp. 217–224.
- [5] F. Mainardi, Fractional calculus: some basic problems in continuum and statistical mechanics. Springer, 1997.
- [6] A. H. Bokhari, A. H. Kara, and F. D. Zaman, "On the solutions and conservation laws of the model for tumor growth in the brain," J. Math. Anal. Appl., vol. 350, no. 1, pp. 256–261, 2009.
- [7] I. M. Sokolov, J. Klafter, and A. Blumen, "Fractional kinetics," Phys. Today, vol. 55, no. 11, pp. 48–54, 2002.
- [8] R. Metzler and J. Klafter, "The random walk's guide to anomalous diffusion: a fractional dynamics approach," Phys. Rep., vol. 339, no. 1, pp. 1–77, 2000.
- [9] I. M. Sokolov, J. Klafter, and A. Blumen, "Ballistic versus diffusive pair dispersion in the Richardson regime," Phys. Rev. E, vol. 61, no. 3, p. 2717, 2000.
- [10] W. Chen, "A speculative study of 2/3-order fractional Laplacian modeling of turbulence: Some thoughts and conjectures," Chaos An Interdiscip. J. Nonlinear Sci., vol. 16, no. 2, 2006.
- [11] D. Baleanu, H. Mohammadi, and S. Rezapour, "A fractional differential equation model for the COVID-19 transmission by using the Caputo-Fabrizio derivative," Adv. Differ. equations, vol. 2020, no. 1, p. 299, 2020.
- [12] S. Kumar, J. Cao, and M. Abdel-Aty, "A novel mathematical approach of COVID-19 with non-singular fractional derivative," Chaos, Solitons & Fractals, vol. 139, p. 110048, 2020.
- [13] M. Ali Dokuyucu, E. Celik, H. Bulut, and H. Mehmet Baskonus, "Cancer treatment model with the Caputo-Fabrizio fractional derivative," Eur. Phys. J. Plus, vol. 133, pp. 1–6, 2018.
- [14] M. A. Khan, Z. Hammouch, and D. Baleanu, "Modeling the dynamics of hepatitis E via the Caputo–Fabrizio derivative," Math. Model. Nat. Phenom., vol. 14, no. 3, p. 311, 2019.
- [15] T. H. Solomon, E. R. Weeks, and H. L. Swinney, "Observation of anomalous diffusion and Lévy flights in a two-dimensional rotating flow," Phys. Rev. Lett., vol. 71, no. 24, p. 3975, 1993.
- [16] A. V Chechkin, R. Gorenflo, and I. M. Sokolov, "Fractional diffusion in inhomogeneous media," J. Phys. A. Math. Gen., vol. 38, no. 42, p. L679, 2005.

[17] Q. Du, J. S. Hesthaven, C. Li, C.-W. Shu, and T. Tang, "Preface to the Focused Issue on Fractional Derivatives and General Nonlocal Models," Commun. Appl. Math. Comput., vol. 1, pp. 503–504, 2019.

- [18] A. A. Kilbas, H. M. Srivastava, and J. J. Trujillo, Theory and applications of fractional differential equations, vol. 204. elsevier, 2006.
- [19] J. M. Cruz-Duarte, J. Rosales-Garcia, C. R. Correa-Cely, A. Garcia-Perez, and J. G. Avina-Cervantes, "A closed form expression for the Gaussian-based Caputo-Fabrizio fractional derivative for signal processing applications," Commun. Nonlinear Sci. Numer. Simul., vol. 61, pp. 138–148, 2018.
- [20] H. Ding and C. Li, "Numerical Algorithms for the Fractional Diffusion-Wave Equation with Reaction Term," in Abstract and applied analysis, Wiley Online Library, 2013, p. 493406.
- [21] Z. Avazzadeh, V. R. Hosseini, and W. Chen, "Radial basis functions and FDM for solving fractional diffusion-wave equation," Iran. J. Sci., vol. 38, no. 3, pp. 205–212, 2014.
- [22] M. M. Khader and M. H. Adel, "Numerical solutions of fractional wave equations using an efficient class of FDM based on the Hermite formula," Adv. Differ. Equations, vol. 2016, pp. 1–10, 2016.
- [23] A. Chatterjee, U. Basu, and B. N. Mandal, "Numerical algorithm based on Bernstein polynomials for solving nonlinear fractional diffusion-wave equation," Int. J. Adv. Appl. Math. Mech, vol. 5, no. 2, pp. 9–15, 2017.
- [24] M. R. Hooshmandasl, M. H. Heydari, and C. Cattani, "Numerical solution of fractional sub-diffusion and time-fractional diffusion-wave equations via fractional-order Legendre functions," Eur. Phys. J. Plus, vol. 131, pp. 1–22, 2016.
- [25] U. Ali, A. Iqbal, M. Sohail, F. A. Abdullah, and Z. Khan, "Compact implicit difference approximation for time-fractional diffusion-wave equation," Alexandria Eng. J., vol. 61, no. 5, pp. 4119–4126, 2022.
- [26] F. Zhou and X. Xu, "Numerical Solution of Time-Fractional Diffusion-Wave Equations via Chebyshev Wavelets Collocation Method," Adv. Math. Phys., vol. 2017, no. 1, p. 2610804, 2017.
- [27] F. Zeng, "Second-order stable finite difference schemes for the time-fractional diffusion- wave equation," J. Sci. Comput., vol. 65, no. 1, pp. 411–430, 2015.
- [28] A. V Pskhu, "The fundamental solution of a diffusion-wave equation of fractional order," Izv. Math., vol. 73, no. 2, p. 351, 2009.
- [29] Y. Povstenko, "Neumann boundary-value problems for a time-fractional diffusion-wave equation in a half-plane," Comput. Math. with Appl., vol. 64, no. 10, pp. 3183–3192, 2012.
- [30] J. Ren and Z.-Z. Sun, "Efficient numerical solution of the multi-term time fractional diffusion-wave equation," East Asian J. Applied Math., vol. 5, no. 1, pp. 1–28, 2015.
- [31] N. H. Sweilam, M. M. Khader, and A. M. S. Mahdy, "Crank-Nicolson finite difference method for solving time-fractional diffusion equation," J. Fract. Calc. Appl., vol. 2, no. 2, pp. 1–9, 2012.
- [32] V. Daftardar-Gejji and S. Bhalekar, "Solving fractional diffusion-wave equations using a new iterative method," Fract. Calc. Appl. Anal., vol. 11, no. 2, p. 193, 2008.

[33] M. Garg and P. Manohar, "Numerical solution of fractional diffusion-wave equation with two space variables by matrix method," Fract. Calc. Appl. Anal., vol. 13, no. 2, pp. 191–207, 2010.

- [34] M. M. Khader, "On the numerical solutions for the fractional diffusion equation," Commun. Nonlinear Sci. Numer. Simul., vol. 16, no. 6, pp. 2535–2542, 2011.
- [35] M. H. Heydari, M. R. Hooshmandasl, F. M. M. Ghaini, and C. Cattani, "Wavelets method for the time fractional diffusion-wave equation," Phys. Lett. A, vol. 379, no. 3, pp. 71–76, 2015.
- [36] M. Yaseen, M. Abbas, T. Nazir, and D. Baleanu, "A finite difference scheme based on cubic trigonometric B-splines for a time fractional diffusion-wave equation," Adv. Differ. Equations, vol. 2017, pp. 1–18, 2017.
- [37] J. R. Poulin, Calculating infinite series using Parseval's identity. The University of Maine, 2020.
- [38] N. Khalid, M. Abbas, M. K. Iqbal, and D. Baleanu, "A numerical investigation of Caputo time fractional Allen–Cahn equation using redefined cubic B-spline functions," Adv. Differ. Equations, vol. 2020, no. 1, p. 158, 2020.
- [39] M. Shafiq, M. Abbas, K. M. Abualnaja, M. J. Huntul, A. Majeed, and T. Nazir, "An efficient technique based on cubic B-spline functions for solving time-fractional advection diffusion equation involving Atangana–Baleanu derivative," Eng. Comput., vol. 38, no. 1, pp. 901–917, 2022.
- [40] W. E. Boyce, R. C. DiPrima, and D. B. Meade, Elementary differential equations and boundary value problems. John Wiley & Sons, 2021.
- [41] M. K. Kadalbajoo and P. Arora, "B-spline collocation method for the singular- perturbation problem using artificial viscosity," Comput. Math. with Appl., vol. 57, no. 4, pp. 650–663, 2009.
- [42] C. A. Hall, "On error bounds for spline interpolation," J. Approx. theory, vol. 1, no. 2, pp. 209–218, 1968.
- [43] C. de Boor, "On the convergence of odd-degree spline interpolation," J. Approx. theory, vol. 1, no. 4, pp. 452–463, 1968.
- [44] M. Shafiq, F. A. Abdullah, M. Abbas, A. Sm Alzaidi, and M. B. Riaz, "Memory effect analysis using piecewise cubic B-spline of time fractional diffusion equation," Fractals, vol. 30, no. 08, p. 2240270, 2022.
- [45] M. Abbas, A. A. Majid, A. I. M. Ismail, and A. Rashid, "The application of cubic trigonometric B-spline to the numerical solution of the hyperbolic problems," Appl. Math. Comput., vol. 239, pp. 74–88, 2014.
- [46] I. Wasim, M. Abbas, and M. Amin, "Hybrid B-Spline Collocation Method for Solving the Generalized Burgers-Fisher and Burgers-Huxley Equations," Math. Probl. Eng., vol. 2018, no. 1, p. 6143934, 2018.